Reprinted from the Journal of the American Chemical Society, 1994, *116*.

Using Finite Element Analysis To Calculate the Shapes of Geometrically Confined Drops of Liquid on Patterned, Self-Assembled Monolayers: A New Method To Estimate Excess Interfacial Free Energies $\gamma_{sv} - \gamma_{sl}$

Nicholas L. Abbott,[†] George M. Whitesides,*[,†] Livia M. Racz,[‡] and Julian Szekely*[,‡]

Contribution from the Department of Chemistry, Harvard University, Cambridge, Massachusetts 02138, and Department of Materials Science and Engineering, Massachusetts Institute of Technology, Cambridge, Massachusetts 02139

Received April 14, 1993[⊗]

Abstract: Drops of normal alkanes ($CH_3(CH_2)_nCH_3$, $n = 7$–14) were confined to specific, geometrically defined areas of a surface by patterning the surface with wetting and nonwetting regions. Each region of the surface comprised a self-assembled monolayer (SAM) of an alkanethiolate on gold, with wettable regions formed from $CH_3NHCO(CH_2)_{15}SH$ and nonwetting regions formed from $CF_3(CF_2)_9(CH_2)_2SH$. The asymmetric shapes formed by the geometrically confined drops of liquid were calculated using a finite element analysis that minimized the excess surface free energy and gravitational potential energy of the drop. A calculation started with the area and shape of the wettable region of the surface, the volume of the drop, the liquid–vapor free energy, γ_{lv}, and an *assumed* value of the difference between the solid–vapor and solid–liquid interfacial free energies, $\gamma_{sv} - \gamma_{sl}$. The value of $\gamma_{sv} - \gamma_{sl}$ was adjusted iteratively to fit calculated drop shapes to experimental drop shapes. This combination of experiment and numerical analysis forms the basis of a new method to estimate values of $\gamma_{sv} - \gamma_{sl}$ (and thus, using these values, to calculate the contact angles, θ, that would be observed for unbounded drops) for liquids on organic surfaces. Estimates of θ in the range $15° < \theta < 30°$ were confirmed using a conventional optical telescope and goniometer; estimates in the range $3° < \theta < 15°$ were beyond the resolution of the telescope and goniometer.

Introduction

This paper reports a new experimental method for constructing complex, non-axisymmetric shapes from drops of liquid by constraining their perimeters. A finite element method is used to analyze the shapes of these geometrically confined drops, and the combination of finite element analysis and experimental measurement of drop shape is used to estimate $\gamma_{sv} - \gamma_{sl}$ (where γ_{sv} and γ_{sl} are the excess free energies of the solid–vapor interface and solid–liquid interface, respectively). These results demonstrate the usefulness of patterned, self-assembled monolayers (SAMs) of organic molecules in controlling the formation of complex shapes from liquids, the value of finite element analyses in predicting these shapes, and an application of this combination to obtain experimental estimates of interfacial free energy terms having values in a previously inaccessible (or difficultly accessible) range.

The experimental method relies on confining a drop of liquid to a triangular region of a surface, where one interior angle of the triangle is less than 20°. The small interior angle causes the shape of the confined drop to be sensitive to the excess (specific) free energies of three types of interfaces: solid–liquid (γ_{sl}), liquid–vapor (γ_{lv}), and solid–vapor (γ_{sv}). The top view of the confined drop is especially sensitive to the interfacial free energies and permits estimation of contact angles between liquid and solid as small as 3°.

Self-assembled monolayers (SAMs) formed by the chemisorption of alkanethiols from solution onto gold surfaces[1] have been used in studies of wetting,[2] adhesion,[3] X-ray-induced damage,[4] and electron transfer.[5] Here we confine liquid to a triangular and wettable region of a surface by three intersecting micrometer-wide lines that support nonwettable SAMs.[6] The procedure for generating these patterned surfaces has three steps: (i) formation of an initial self-assembled monolayer of alkanethiolate on the surface of a film of gold by the chemisorption of an alkanethiol from solution; (ii) generation of micrometer-wide lines of bare gold in the SAM by micromachining; and (iii) formation of a second SAM on these micromachined lines. We

[†] Harvard University.
[‡] Massachusetts Institute of Technology.
[⊗] Abstract published in *Advance ACS Abstracts,* December 1, 1993.

(1) *Formation*: Nuzzo, R. G.; Allara, D. L. *J. Am. Chem. Soc.* **1983,** *105,* 4481–4483. Nuzzo, R. G.; Fusco, F. A.; Allara, D. L. *J. Am. Chem. Soc.* **1987,** *109,* 2358–2368. Bain, C. D.; Troughton, E. B.; Tao, Y.-T.; Evall, J.; Whitesides, G. M. Nuzzo, R. G. *J. Am. Chem. Soc.* **1989,** *111,* 321–335. Whitesides, G. M.; Laibinis, P. E. *Langmuir* **1990,** *6,* 87–96 and references cited therein.

(2) *Wetting*: Bain, C. D.; Whitesides, G. M. *J. Am. Chem. Soc.* **1988,** *110,* 5897–5898. Bain, C. D.; Whitesides, G. M. *Langmuir* **1989,** *5,* 1370–1378. Dubois, L. H.; Zegarski, B. R.; Nuzzo, R. G. *J. Am. Chem. Soc.* **1990,** *112,* 570–579. Laibinis, P. E.; Whitesides, G. M. *J. Am. Chem. Soc.* **1992,** *114,* 1990–1995.

(3) *Adhesion*: Allara, D. L.; Hebard, A. F.; Padden, F. J.; Nuzzo, R. G.; Falcone, D. R. *J. Vac. Sci. Technol., A* **1983,** 376–382. Stewart, K. R.; Whitesides, G. M.; Godfried, H. P.; Silvera, I. F. *Rev. Sci. Instrum.* **1986,** 57, 1381–1383. Czanderna, A. W.; King, D. E.; Spaulding, D. *J. Vac. Sci. Technol., A.* **1991,** *9,* 2607–2613. Armstrong, F. A.; Hill, H. A. O.; Walton, N. J. *Acc. Chem. Res.* **1988,** *21,* 407–413. Pale-Grosemange, C.; Simon, E. S.; Prime, K. L.; Whitesides, G. M. *J. Am. Chem. Soc.* **1991,** *113,* 12–20. Haussling, L.; Michel, B.; Ringsdorf, H.; Rohrer, H. *Angew. Chem., Int. Ed. Engl.* **1991,** *30,* 569–572. Tarlov, M. J.; Bowden, E. F. *J. Am. Chem. Soc.* **1991,** *113,* 1847–1849. Prime, K. L.; Whitesides, G. M. *Science (Washington, D. C.)* **1991,** *252,* 1164–1167. Haussling, L.; Ringsdorf, H.; Schmitt, F.-J.; Knoll, W. *Langmuir* **1991,** *7,* 1837–1840. Prime, K. L.; Whitesides, G. M. *J. Am. Chem. Soc.*, submitted for publication.

(4) *X-ray Induced Damage*: Bain, C. D. Ph.D. Thesis, Harvard University, 1988. Laibinis, P. E.; Graham, R. L.; Biebuyck, H. A.; Whitesides, G. M. *Science (Washington, D. C.)* **1991,** *254,* 981–983.

(5) *Electron Transfer*: (a) Sabatini, E.; Rubinstein, I. *J. Phys. Chem.* **1987,** *91,* 6663–6669. (b) Porter, M. D.; Bright, T. B.; Allara, D. L.; Chidsey, C. E. D. *J. Am. Chem. Soc.* **1987,** *109,* 3559–3568. Chidsey, C. E. D.; Loiacono, D. N. *Langmuir* **1990,** *6,* 682–691. Chidsey, C. E. D.; Bertozzi, C. R.; Putvinski, T. M.; Mujsce, A. M. *J. Am. Chem. Soc.* **1990,** *112,* 4301–4306. Miller, C.; Cuendet, P.; Gratzel, M. *J. Phys. Chem.* **1991,** *95,* 877–886. Hickman, J. J.; Ofer, D.; Zou, C. F.; Wrighton, M. S.; Laibinis, P. E.; Whitesides, G. M. *J. Am. Chem. Soc.* **1991,** *113,* 1128–1132. Miller, C.; Gratzel, M. *J. Phys. Chem.* **1991,** *95,* 919–922. Finklea, H. O.; Hanshew, D. D. *J. Am. Chem. Soc.* **1992,** *114,* 3175–3181 and references cited therein.

(6) Abbott, N. L. ; Folkers, J. P.; Whitesides, G. M. *Science* **1992,** 257, 1380–1382.

0002-7863/94/1516-0290$04.50/0

used this procedure to prepare triangular areas of a SAM formed from $CH_3NHCO(CH_2)_{15}SH$, where the perimeter of the triangle is defined by lines of an oleophobic SAM formed from $CF_3(CF_2)_9(CH_2)_2SH$. Self-assembled monolayers formed from $CH_3NHCO(CH_2)_{15}SH$ and $CF_3(CF_2)_9(CH_2)_2SH$ were used because drops of normal alkanes ($CH_3(CH_2)_nCH_3$, $n = 7$–14) do not wet SAMs formed from $CF_3(CF_2)_9(CH_2)_2SH$ and because we estimated (see below) the contact angles of alkanes on SAMs formed from $CH_3NHCO(CH_2)_{15}SH$ covered the full range of interest between 3° and 30°, depending on the length of the alkane chain.

We used a finite element method[7] to calculate the shapes of the confined drops by minimizing their excess free energy. In the problems of interest here, the excess free energy is the sum of gravitational potential energy and excess surface free energy. For reasons discussed later (see the Results and Discussion section) we do not believe that "line tensions"[8,9] make an important contribution to the excess free energy of the systems that we have investigated. The excess free energy of the system was minimized subject to the constraint of a known, constant volume of liquid and the geometrical constraints imposed by the nonwetting perimeter of the triangle. Values of $\gamma_{sv} - \gamma_{sl}$, which are required for the calculation of the excess surface free energy in the finite element method and which are unknown initially, were adjusted to match the experimentally measured and calculated shapes of the confined drops. Because shapes formed by three-phase contact lines of drops in corners of triangles were found to be sensitive measures of $\gamma_{sv} - \gamma_{sl}$ and because these shapes could be described using a single length d (see eq 3), comparisons of d, calculated and measured, formed the basis of the method for estimating $\gamma_{sv} - \gamma_{sl}$. The contact angle of each alkane on a SAM formed from $CH_3NHCO(CH_2)_{15}SH$ was calculated from the estimated value of $\gamma_{sv} - \gamma_{sl}$, γ_{lv} (taken from the literature[10]), and Youngs equation:[11]

$$\cos\theta = (\gamma_{sv} - \gamma_{sl})/\gamma_{lv} \quad (1)$$

Contact angles calculated from eq 1 predict the behavior of an *unbounded* drop: Young's equation does not apply to a drop confined by a nonwetting groove.

To verify this new method of estimating contact angles (which we refer to as the "bounded-drop method"), we compared our estimates of contact angles larger than 15° ($15° < \theta < 30°$) with measurements obtained from unbounded drops of liquid alkanes using a conventional telescope and goniometer.[12] We found good agreement and infer from this agreement that our method of estimating contact angles is accurate over this range of contact angles, at least. We believe that the method will also be valid for smaller contact angles but have not verified this belief experimentally. Contact angles less than 15° ($3° < \theta < 15°$) are too small to be measured using a contact angle goniometer. The ability of the bounded drop method to provide estimates of contact angles in this range allows access to values that are either difficult or impractical to measure using a conventional telescope and goniometer. An alternative method for measuring small contact angles is interference microscopy.[13] The bounded-drop method, however, does not require any particular experimental apparatus; it requires only the measurement of macroscopic lengths that can be seen with the naked eye. It is also generally applicable to all liquids (including those liquids that are opaque).

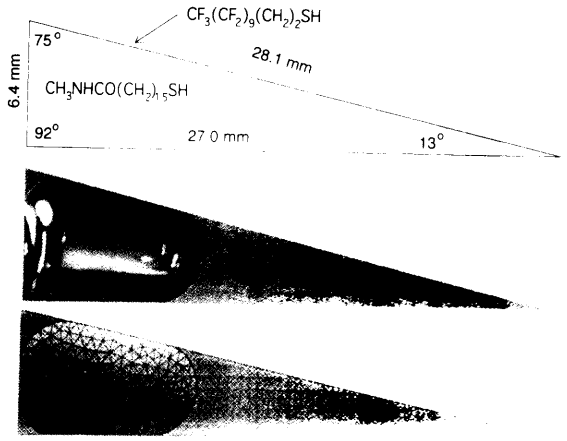

Figure 1. (a, top) Diagram of a representative triangular pattern generated on a gold film using SAMs of different wettability: micrometer-wide lines of the SAM formed from $CF_3(CF_2)_9(CH_2)_2SH$ bound a triangular domain of the SAM formed from $CH_3NHCO(CH_2)_{15}SH$. (b, middle) Top view (photograph) of a 20-μL drop of hexadecane ($CH_3(CH_2)_{14}CH_3$) confined within the triangular boundary shown in part a. (c, bottom) Calculated (see Numerical Analysis section) shape (top view) of a 20-μL drop of hexadecane confined within the triangular boundary shown in part a. For the calculation, $\gamma_{lv} = 27.0$ dyn/cm, $\gamma_{sv} - \gamma_{sl} = 23.6$ dyn/cm (corresponding to $\theta = 29°$), and $\rho_l = 0.773$ g/cm^3.

Experimental Measurements

We measured the shapes formed by liquid confined to a triangular area of a surface because (i) the edges of triangles are constructed from straight lines and, therefore, are easy to make using the experimental procedure outlined in the Introduction, (ii) the interior angle of one corner of each triangle can be made to be small (≈10°) (the small interior angle is necessary to estimate small contact angles), and (iii) the shapes of the drops confined within each triangle can be readily analyzed using the finite element method to yield the $\gamma_{sv} - \gamma_{sl}$ (and to provide estimates of the contact angle, θ) characterizing these interfaces. The triangular areas were constructed from a SAM formed from $CH_3NHCO(CH_2)_{15}SH$ and surrounded by an oleophobic SAM formed from $CF_3(CF_2)_9(CH_2)_2SH$ (see Figure 1a). Because contact angles of liquid alkanes on SAMs formed from $CF_3(CF_2)_9(CH_2)_2SH$ ($\theta \sim 90$–110°) are larger than those on SAMs formed from $CH_3NHCO(CH_2)_{15}SH$ ($\theta \sim 3$–30°), drops of alkanes do not spread across the SAM formed from $CF_3(CF_2)_9(CH_2)_2SH$. The drops are confined to the triangular area defined by the SAM formed from $CH_3NHCO(CH_2)_{15}SH$.

The first step in the preparation of the triangular pattern was to cover a gold film evaporated onto a silicon wafer with a SAM formed from a solution of $CH_3NHCO(CH_2)_{15}SH$ in ethanol. The second step was to micromachine bare gold grooves into the SAM using a 3 mN (0.30 g) load applied to the tip of a surgical scalpel. Scanning electron micrographs (SEMs) of the grooves showed plastic deformation of the gold film; this observation suggests the pressure at the tip of the scalpel exceeded the yield strength of the gold.[6] We estimate this pressure to be 300 MPa (assuming an area of scalpel tip of 10 μm^2 in contact with the Au surface and a measured load of 3 mN); this value is greater than the yield strength of bulk gold (3.4–14 MPa, depending on the thermal history) and comparable to the ultimate tensile strength of bulk gold (131 MPa).[14] Energy-dispersive X-ray fluorescence measurements did not detect Si within the micromachined grooves. The third and final step of the patterning

(7) The name of the public domain computer code is Surface Evolver. It is under development by K. A. Brakke as a part of the Geometry Center, University of Minnesota, which is sponsored by the National Science Foundation and the Minnesota Supercomputer Institute. Further details can be found in the Surface Evolver manual or the function **iterate()** in the source code, both of which are available to the public by anonymous file transfer protocol.

(8) A "line tension" can arise from local variations in the energy content of interfaces in the vicinity of a three-phase contact line.

(9) de Gennes, P. G. *Rev. Mod. Phys.* **1985**, *57*, 827.

(10) Jasper, J. J. *J. Phys. Chem. Ref. Data* **1972**, *1*, 841–1009.

(11) Young, T. *Philos. Trans. R. Soc. London* **1805**, *95*, 65.

(12) This method relies on the direct observation and measurement of the contact angle between a liquid and a surface using a telescope and goniometer. This measurement is difficult and inaccurate for contact angles of approximately 15° or less.

(13) Callaghan, I. C.; Everett, D. H.; Fletcher, A. J. P. *J. Chem. Soc., Faraday Trans. 1* **1983**, *79*, 2723–2728.

(14) Wise, E. M. *Gold Recovery, Properties, and Applications*; Van Nostrand: New York, 1964.

process was the formation of a second SAM on the micromachined grooves of bare gold. The regions of bare gold were selectively functionalized by exposing the first SAM and micromachined grooves to a solution of 0.1 mM $CF_3(CF_2)_9(CH_2)_2SH$ in isooctane for 20 s.[15] The advancing contact angle of hexadecane on a SAM formed from $CH_3NHCO(CH_2)_{15}SH$ (29°) was not changed after immersion of the SAM in a 0.1 mM solution of $CF_3(CF_2)_9(CH_2)_2$-SH for 20 s.

Confined drops of alkanes were prepared by delivering a known volume (typically 10–20 ± 0.1 μL) of liquid alkane to the centroid (estimated by eye) of the triangular area of the SAM formed from $CH_3NHCO(CH_2)_{15}SH$. Gravitational and interfacial forces caused each drop to spread across the surface until the minimum energy of the drop was reached within the confines of the triangular area. We observed an upper limit on the volume of liquid confined by the nonwetting boundaries of the triangle. This limiting volume of liquid was influenced by the advancing contact angle of the liquid on the SAM that formed the boundary of the triangle. For example, micromachined grooves formed with a machining load of 3 mN and covered with a SAM formed from CH_3NHCO-$(CH_2)_{15}SH$ did not confine drops of alkane to the triangular area. Grooves formed with larger loads (>10 mN) and covered with a SAM formed from $CH_3NHCO(CH_2)_{15}SH$ did show a weak tendency to pin drops. Because larger loads produce larger grooves, we conclude the shape of the groove can influence the wetting of liquids on the grooves. These observations are consistent with the known influence of "surface roughness" (including grooves) on the wetting of solid surfaces with liquids.[9]

We observed that liquids confined to the triangular areas did not, in general, spread all the way into the corners of the triangle. Because wetting in the corners of triangles changed with the type of liquid and was a sensitive measure of the overall shapes of the drops, we compared top views of each drop in the corners of the triangle to the predictions of the finite element analysis to obtain estimates of the contact angles of the liquid on the surface. We do not report side profiles of the drops because, for values of $(\gamma_{sv} - \gamma_{sl})/\gamma_{lv} \approx 1$, the heights of the films of liquid were ~100 μm and are much less sensitive to changes in $\gamma_{sv} - \gamma_{sl}$ than are the shapes of the drops in the corners of the triangles. Other measures of shape, such as the total length of the perimeter of the drop, are also insensitive measures of changes in $\gamma_{sv} - \gamma_{sl}$.[16] The contact angles calculated for unbounded drops using values of $\gamma_{sv} - \gamma_{sl}$ obtained from the numerical method with bounded drops correspond to "advancing" contact angles, because the experimental drop shapes were formed by liquid advancing into the corners of the triangle.

Contact angles estimated by the finite element analysis and eq 1 and found to be larger than 15° were compared to advancing contact angles directly measured on unbounded drops using a conventional goniometer and optical telescope. This comparison allowed us to assess the accuracy of the bounded-drop method for estimating contact angles over the range accessible by direct measurement ($\theta > 15°$).

Numerical Analysis

The public domain computer code Surface Evolver[7] was used to simulate the shapes formed by drops of liquid confined to triangular areas. We used Surface Evolver to seek the shape of the drop for which the excess free energy of the system (drop of liquid and surface), F, was minimized. Two energy components were considered, an excess surface free energy and a gravitational potential energy (eq 2). In this equation, ρ is the density of the

$$F = A_{sv}\gamma_{sv} + A_{lv}\gamma_{lv} + A_{sl}\gamma_{sl} + \int \rho g z \, dV \qquad (2)$$

liquid, g is the gravitational acceleration, and z is the vertical position of a differential volume of fluid, dV.

The physical parameters required for calculation of the minimum-energy shape of a drop of liquid confined to a triangular area are (i) the dimensions and angles of the triangle, (ii) the volume of the drop, (iii) the density of the liquid, and (iv) the interfacial free energies, γ_{lv} and $\gamma_{sv} - \gamma_{sl}$. Only the *difference* $\gamma_{sv} - \gamma_{sl}$ and the value γ_{lv} are required because the area of the triangle, $A_{sv} + A_{sl}$, is constant.[17] The gravitational term (the last term in eq 2) was calculated from the volume and shape of the drop and the density of the liquid.

Surface Evolver models a surface as a collection of oriented triangular facets connected by their edges, with the edges meeting at vertices (Figure 2). At the beginning of the analysis, each facet was assigned the free energy, γ_{lv}, γ_{sv}, or γ_{ls} depending on the type of facet. We assumed the value of each free energy was independent of position on the drop. The initial state of the drop was arbitrarily taken to be a cube of liquid placed at the centroid of the triangle (Figure 2a). Each side of the drop was divided into four triangular facets. The final shape of the drop was independent of the specified initial shape and position of the drop. The energy of the drop was minimized at each iteration of the search by calculating the force on each vertex. The vertex was then moved by a scaled factor of the force where the scaling factor was calculated (i) to maximize the decrease in the energy of the drop and (ii) to satisfy the necessary physical constraints on the system (such as boundary conditions[18] and conservation of liquid volume). The sizes of the facets were refined during the energy minimization (at the discretion of the user) whenever the positions of the facets of the drop were invariant. The details can be found in the Surface Evolver manual.[7]

Local minima in the energy of the drop were encountered during the energy minimization, and "jiggling"—displacing the surface of the drop by a set fraction, again at the discretion of the user, of its size—was used to perturb the drop away from the local minima in search of the global energy minimum. We have used both conjugate gradient and steepest descent methods of energy minimization (both are available within Surface Evolver[7]). It was useful to employ both methods because the steepest decent method is robust but converges slowly, whereas the conjugate gradient method can lead to fast convergence but is less stable. The energy minimization proceeded until the positions of the facets comprising the surface of the drop and the total energy of each drop were stationary (to 1 part in 10^5) between iterations. Surface Evolver was executed on a workstation (Sun SPARC-station 2). Typical convergence times ranged from ~10 min for contact angles greater than 40° to ~8 h for contact angles less than 5°.

Results and Discussion

Figure 1b shows a top view of a 20-μL drop of hexadecane confined within the triangular area of the surface shown in Figure 1a. The hexadecane did not spread completely into the corners of the triangle. In each corner of the triangle, the three-phase

(15) The rate of reaction of $CF_3(CF_2)_9(CH_2)_2SH$ with bare gold is faster by a factor of 10 than the rate of its exchange into the first SAM [Reference 3 above. Chidsey, C. E. D.; Bertozzi, C. R.; Putvinski, T. M.; Mujsce, A. M. *J. Am. Chem. Soc.* **1990**, *112*, 4301. Collard, D. M.; Fox, M. A. *Langmuir* **1991**, *7*, 1192. Bain, C. D.; Biebuyck, H. A.; Whitesides, G. M. *Langmuir* **1989**, *5*, 723.]. By using a dialkyl disulfide to form the second SAM, the exchange with thiolates of the first SAM can be reduced to less than 0.1% [Biebuyck, H. A.; Whitesides, G. M. Unpublished results]. We did not use $[CF_3(CF_2)_9(CH_2)_2S]_2$ to form the second SAM because of its insolubility in isooctane.

(16) The total length of the perimeter of a confined drop is dominated by the portion bounded by the nonwetting groove and is not, therefore, a sensitive measure of small changes in the shape of a drop.

(17) The area within the triangle is $A_t = A_{sv} + A_{sl}$. This equation can be used to reexpress the contribution of the surface energy to the total energy of the system as $\gamma_{lv}A_{lv} + \gamma_{sl}A_{sl} + \gamma_{sv}A_{sv} = \gamma_{lv}A_{lv} + \gamma_{sl}(A_t - A_{sv}) + \gamma_{sv}A_{sv} = A_{sv}(\gamma_{sv} - \gamma_{sl}) + \gamma_{lv}A_{lv} + A_t\gamma_{sl}$. Because the term $A_t\gamma_{sl}$ is not a function of the shape of the drop, the contribution of the surface energy to the total energy of the system is seen to be a function of only $\gamma_{sv} - \gamma_{sl}$ and γ_{lv}.

(18) We have treated the boundary conditions in the numerical analysis as impenetrable lines. The description of the lines formed from $CF_3(CF_2)_9$-$(CH_2)_2SH$ as impenetrable lines is valid for contact angles exceeding 90°. In this case, the base of the drop will be constrained at the nonwetting line and the surface of the drop can extend over and above the line.

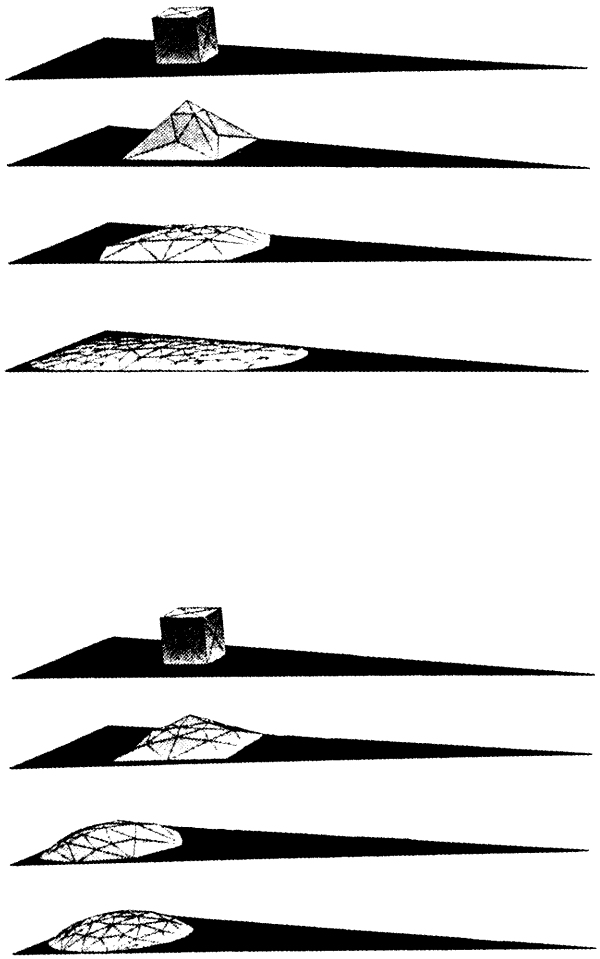

Figure 2. Calculated shapes of drops of liquid confined to triangular areas during energy (surface and gravitational) minimization. For both calculations the initial shape of the drop was a cube, the subsequent shapes are intermediate shapes, and the final shape of the drop that is shown is the (equilibrium) shape corresponding to the calculated minimum in energy. The center of mass of the drop shown in part b has moved during the energy minimization. The lengths of the sides of the triangle are (in mm) 27.2, 27.0, and 8.1, and the opposite interior angles (in degrees) are 82, 81, and 17. The parameter values used in the simulation were as follows: (a, top) γ_{lv} = 24.9 dyn/cm, $\gamma_{sv} - \gamma_{sl}$ = 24.4 dyn/cm (corresponding to a contact angle of 11.2°), ρ_l = 0.75 g/cm^3, V = 15 μl; (b, bottom) γ_{lv} = 24.9 dyn/cm, $\gamma_{sv} - \gamma_{sl}$ = 19.1 dyn/cm (corresponding to a contact angle of 40°), ρ_l = 0.75 g/cm^3, V = 15 μl. Details of the numerical simulation are given in the Numerical Analysis section.

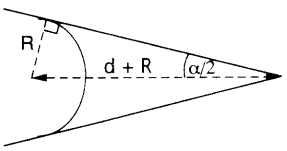

Figure 3. Schematic illustration of the meniscus of a drop that has partially spread into an interior angle of a triangle.

contact line[19] is circular, tangent to each side of the triangle, and has a radius R. We have defined the shortest distance from the three-phase contact line to the smallest interior corner of the triangle to be d (Figure 3). The quantities d and R are related by eq 3; this relation was confirmed by experimental observation.

$$\frac{d}{R} = \frac{1 - \sin(\alpha/2)}{\sin(\alpha/2)} \qquad (3)$$

Here, α is the interior angle of the triangle. Equation 3 can be derived from trigonometry by considering the three-phase contact line to be circular and tangent to each side of the triangle (i.e. $\sin(\alpha/2) = R/R + d$ in Figure 3).

(19) The three-phase contact line is the line that defines the intersection of the liquid, air, and solid phases.

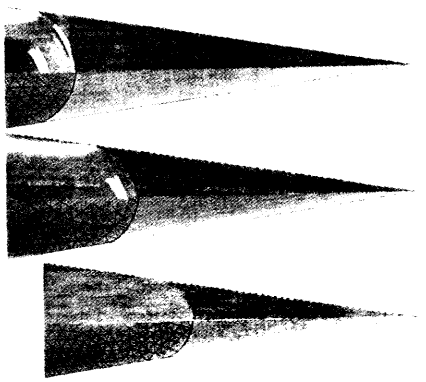

Figure 4. Geometrically confined 15-μL drops of alkanes ($CH_3(CH_2)_n$-CH_3, n = 8–10) partially spread into the corner of a triangular boundary constructed from micrometer-wide lines of the SAM formed from $CF_3(CF_2)_9(CH_2)_2SH$. For clarity, the behavior of the drop is only shown in the corner of the triangle with the smallest angle (17°). The top half of each image is a photograph, and the bottom half shows the result of the finite element analysis. The surface of the triangular domain is a SAM formed from $CH_3NHCO(CH_2)_{15}SH$. The following values of parameters were used for the simulations: (a, top) decane γ_{lv} = 23.4 dyn/cm, $\gamma_{sv} - \gamma_{sl}$ = 23.1 dyn/cm (corresponding to θ = 8.6°), ρ_l = 0.730 g/cm^3; (b, middle) undecane γ_{lv} = 24.2 dyn/cm, $\gamma_{sv} - \gamma_{sl}$ = 23.7 dyn/cm (corresponding to θ = 11.2°), ρ_l = 0.740 g/cm^3; (c, bottom) dodecane γ_{lv} = 24.9 dyn/cm, $\gamma_{sv} - \gamma_{sl}$ = 23.8 dyn/cm (corresponding to θ = 17.4°), ρ_l = 0.750 g/cm^3.

Figure 1c shows the shape of a 20-μL drop of hexadecane calculated using the finite element analysis. For this calculation, γ_{lv} (27.0 dyn/cm) was a literature value,[10] and $\gamma_{sv} - \gamma_{sl}$ (23.6 dyn/cm) was estimated by measuring the advancing contact angle of an unbounded drop of hexadecane on a SAM formed from $CH_3NHCO(CH_2)_{15}SH$ (θ = 29°) and using eq 1. The experimentally observed (Figure 1b) and calculated (Figure 1c) shapes of the drops are in good qualitative agreement, at least. This agreement suggests that the numerical analysis describes the important components of the free energy of the system. A contribution from "line tension"[8,9] at the three-phase contact line to the free energy of the system does not appear to be significant in this system or other systems that we have investigated.[20]

The shapes formed by drops of alkanes confined to triangular areas are influenced by (i) the structure of the alkane, (ii) the volume of the drop of alkane, and (iii) the shape and size of the triangle. Figure 4 summarizes the influence of the structure of the alkane on the shape of the drop. Because the top view of the three-phase contact line provides a sensitive measure of the excess interfacial free energies, we show top views of the meniscus formed by each drop of liquid in the smallest interior angle of the triangle. For drops of alkane with equal volumes, a decrease in the length of the alkane chain causes the drop to spread farther into the corner of the triangle because γ_{lv} decreases with decreasing chain length; γ_{sl} increases with decreasing length of the alkane chain and acts to oppose the experimentally observed influence of the drop shape on the structure of the alkane.

(20) Two pieces of evidence suggest that line tension is not important in determining the macroscopic shapes of drops in the systems that we have investigated. First, we obtained good agreement between the two independent estimates of small contact angles shown in Figure 5: if "line tensions" were an important factor in determining the shapes of the drops, because the lengths of the three-phase contact lines in each of the measurements were different, we would not expect this good agreement. Second, if we assume van der Waals interactions (a good assumption for alkanes), the formalism of de Gennes[9] provides an estimate of the height, h_c, of a liquid film that is perturbed by attractive interactions in the region near the three-phase contact line: $h_c \sim a/\theta_e$, where a is a molecular length ($\sim$10 Å) and θ_e is the macroscopic contact angle ($\theta_e \ll 1$). For a contact angle of 1°, $\theta_e \sim \pi/180$, and $h_c \sim$ 500 Å. Because this estimate of h_c is much smaller than the typical thickness of the films of liquid reported in this paper ($\sim$100 μm; 15 μL of liquid distributed over a surface area of $\sim$100 mm^2), we do not expect to observe the effect of line tensions in our experimental measurements of the drop shapes. In general, thin-film effects are observed for films less than $\sim$1 μm in thickness.

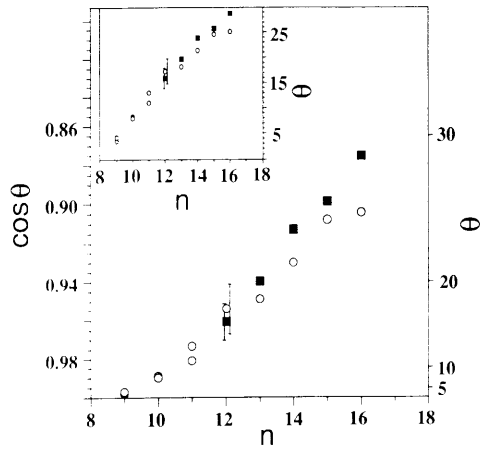

Figure 5. Advancing contact angles, θ, for a series of normal alkanes as a function of the number of carbon atoms in the alkane, n, on a SAM formed from $CH_3NHCO(CH_2)_{15}SH$: (squares) measured using a contact angle goniometer; (circles) estimated using the geometrically confined drop method (see text for details). Contact angles estimated using the bound drop method are "advancing" contact angles because the bounded drops were formed by liquid advancing into the corners of the triangle. Advancing contact angles were also measured using the contact angle goniometer and telescope. Results for two independently prepared SAMs formed from $CH_3NHCO(CH_2)_{15}SH$ are shown for nonane, decane, and undecane.

Figure 5 shows the cosine of the advancing contact angle, θ, for normal alkanes ($CH_3(CH_2)_9CH_3$, where $n = 9$–14) on a SAM formed from $CH_3NHCO(CH_2)_{15}SH$, estimated by the two independent methods: (i) direct measurement with a telescope and goniometer (advancing drop method) and (ii) indirect measurement using the bounded-drop method. Because we observed good agreement between the overall shapes of calculated and experimentally observed three-phase contact lines (Figures 1 and 4) and because we observed the shapes of drops in the corners of triangles to be sensitive measures of small changes in $\gamma_{sv} - \gamma_{sl}$, we found it sufficient to characterize the shape of each drop by a single length d or R; each length, when combined with eq 3, describes the overall shape of a three-phase contact line in the corner of a triangle. The contact angles reported in Figure 5 were estimated by adjusting the value of $\gamma_{sv} - \gamma_{sl}$ to fit calculated values to experimental values of d . We report our results in terms of d because it is more easily measured than R. Figure 5 shows good agreement (typically within 2°) between the two methods of estimating contact angles over the range $15° < \theta < 30°$.

Figure 5 also shows estimates of contact angles for nonane ($\theta = 4°$), decane ($\theta = 8°$), and undecane ($\theta = 12°$), which were determined by the bounded-drop method. For each type of alkane, two independent estimates of contact angle were made using triangular regions of different shape and size. Because the lengths of the three-phase contact lines were different in each of the estimates, we would not have observed the good agreement between estimates (see Figure 5) if factors (for example, line tensions) other than the excess surface free energy and gravitational energy significantly influenced the shapes of the bounded drop. Contact angles in the range $\theta < 15°$ are too small to be accurately measured using a conventional contact angle goniometer. These estimates illustrate the capability of the bounded-drop method to provide contact angles that are either difficult or impractical to measure using a conventional telescope and goniometer.

Conclusions

The most important aspects of this work are (i) the demonstration of *control* over shapes formed from liquids by patterning surfaces with self-assembled monolayers of organic molecules with different wettability and (ii) the *prediction* of the shapes of these drops by minimizing the sum of gravitational and excess surface free energies using a finite element analysis. Because top views of drops confined to corners of patterned surfaces were found to be sensitive measures of wettability and because the shapes of drops in such corners can be described by a single length d, comparisons of calculated and measured values of d formed the basis of a method for estimating the excess surface free energies of liquids on SAMs ($\gamma_{sv} - \gamma_{sl}$) and the corresponding contact angles (θ). In principle, by making one interior angle of the triangle small and by varying the volume of the liquid in the drop, the experimentalist can ensure that the measured length, d, is sensitive to very small changes in $\gamma_{sv} - \gamma_{sl}$ (corresponding to small changes in the contact angle: <1°). We have measured values of $\gamma_{sv} - \gamma_{sl}$ corresponding to contact angles of 3° using values of d of 5 mm. We have not determined the lower limit on the size of the contact angle that can be estimated using the bounded-drop method. We believe, however, that surface inhomogeneities will probably determine this lower limit. For estimates of $\gamma_{sv} - \gamma_{sl}$ corresponding to contact angles less than 15°, one interior angle of the triangle should be made to be smaller than 20°. The bounded-drop method of estimating contact angles is useful because it allows access to a range of values of $\gamma_{sv} - \gamma_{sl}$ and of estimates of contact angles, that are frequently encountered in the study of the physical chemistry of organic interfaces ($3° < \theta < 15°$) but that are difficult to meaure directly using optical goniometers.

Experimental Section

Materials. Titanium (99.999+%), gold (99.999+%), isooctane, and normal alkanes ($CH_3(CH_2)_nCH_3$, $n = 7$–14) were obtained from Aldrich. Isooctane was twice percolated through a column of neutral alumina (EM Science) prior to use. Si(100) wafers (Silicon Sense) were rinsed with absolute ethanol (Quantum Chemical) and dried prior to placement in the evaporation chamber.

Preparation of Gold Films. Titanium (100 Å) and gold (2000 Å) were evaporated in sequence at 5 Å/s onto Si(100) wafers in a cryogenically pumped chamber (base pressure $\approx 8 \times 10^{-8}$ Torr; operating pressure $\approx 1 \times 10^{-6}$ Torr) using an electron beam. The resulting gold films are polycrystalline but have a predominant crystallographic orientation that is (111).

Preparation of SAMs. Self-assembled monolayers were formed on the evaporated films of gold by immersion in 1 mM deoxygenated ethanol solutions of $CH_3NHCO(CH_2)_{15}SH$ for 2 h. Micrometer-wide lines of bare gold were micromachined into the SAM using the tip of a surgical scalpel (Feather Industries). The depth and width of the micromachined grooves could be controlled by varying the load (1.2–9.8 mN) on the tip of the scalpel. The regions of bare gold were covered with a SAM by immersion in an isooctane solution of 0.2 mM $CF_3(CF_2)_9(CH_2)_2SH$ for 20 s.

Wetting. All wetting experiments were carried out in air, with the exception of experiments performed with nonane and decane. Due to the volatility of nonane and decane, these experiments were carried out under atmospheres that had been presaturated with each alkane. Two criteria were met before any measurement was accepted: (i) the three-phase contact line in each corner of the triangle was smooth and symmetric, and (ii) the drop was stationary for a period of 5 min. Drops with small contact angles took up to 15 min to reach a steady state. The samples were washed between measurements with heptane, ethanol, water, and a second wash in heptane and then dried in a stream of dry nitrogen.

Top views of the drops were recorded using a video camera (NEC) and a Macintosh Quadra 700 with a 24 XLTV digitizing video board (RasterOps). Images were captured using the software MediaGrabber 1.7 (RasterOps) and analyzed using Image 1.47 (National Institutes of Health).

Advancing contact angles θ were measured using a telescope and goniometer (Rame-Hart) on both sides of static unbounded drops (~1 μL) that had been delivered to the surface using an electric pipet (Matrix Technologies).

Acknowledgment. This research was supported in part by the Office of Naval Research and by the Defense Advanced Research Projects Agencies. Facilities for surface analysis (SEM and XPS) of the Harvard University Materials Research Laboratory were used in this research. N.L.A. thanks Hans Biebuyck for useful discussions.